We are IntechOpen, the world's leading publisher of Open Access books Built by scientists, for scientists

4,800
Open access books available

122,000
International authors and editors

135M
Downloads

Our authors are among the

154
Countries delivered to

TOP 1%
most cited scientists

12.2%
Contributors from top 500 universities

CLARIVATE ANALYTICS BOOK CITATION INDEX INDEXED

WEB OF SCIENCE™

Selection of our books indexed in the Book Citation Index in Web of Science™ Core Collection (BKCI)

Interested in publishing with us?
Contact book.department@intechopen.com

Numbers displayed above are based on latest data collected.
For more information visit www.intechopen.com

6

InAs Quantum Dots in Symmetric InGaAs/GaAs Quantum Wells

Tetyana V. Torchynska
ESFM-National Polytechnic Institute, Mexico D.F., Mexico

1. Introduction

The self-assembled InAs quantum dots (QDs) are the subject of substantial interest during last fifteen years due to both fundamental scientific and application reasons. In these systems, the strong localization of an electronic wave function leads to an atomic-like electronic density of states and permits to realize the novel and improved photonic and electronic devices. Microlectronic and optoelectronic devices based on quantum wells (QWs) with InAs QDs have been the subject of investigation for the applications in semiconductor lasers for the optical fiber communication [1-3], infrared photo-detectors [4-6], electronic memory devices [7,8], as well as single electron devices and single photon light sources on the base of single-QD structures for the quantum information applications [9-12]. QDs are especially attractive for the applications in semiconductor lasers. For laser or photodiode applications the surface density of QDs has to be high, but for single-QD devices the QD density has to be low. As a result, there is an extensive effort to manipulate and control the position, size, shape and density of QDs [13-19].

Self-assembled InAs/GaAs QDs in lattice-mismatched systems can be achieved by using the Stranski–Krastanow (S–K) growth mode [20-22]. In the process of InAs/GaAs QDs growth using the S–K growth mode, the InAs mismatched layer growths two dimensionally on the GaAs substrate during the initial stage; then, above a critical thickness, the strain increased and the dislocation-free QDs with a three-dimensional shape are formed on a residual two-dimensional wetting layer (WL) [23,24]. InAs/GaAs QD structures grown using the S–K mode have inherent several problems: the density random distribution, the large temperature-dependent variation of the photoluminescence (PL) intensity and line width resulting from the nonuniform size and density of InAs QDs [25] etc. Precise control of the QD size and the homogeneity of InAs QD distribution is necessary for achieving the high-performance devices.

2. Advances of InAs QDs in InGaAs/GaAs quantum wells

InAs/GaAs QDs are especially attractive for the applications in lasers because the QD based lasers have a higher differential gain, lower threshold current density, and improved temperature performance in comparison with QW lasers [1-3]. The band structures of InAs/GaAs QDs are well suited for covering the 1.30 and 1.55 μm spectral ranges, important

in optical fiber communications. These wavelengths are impossible to achieve in quantum well (QW) InAs/GaAs structures due to the strain-limited thicknesses. It is shown that the QD density in laser structures can be enlarged significantly by growing the dots within $In_xGa_{1-x}As/GaAs$ QWs, in so called dot–in-a-well (DWELL) structures [3, 4]. In these structures photoluminescence has been enhanced due to better crystal quality of the layer surrounding QDs and more effective exciton capture into the QW and into QDs.

A crucial aspect for the realization of efficient light-emitting devices operated at room temperature is the understanding of a temperature dependence of QD photoluminescence. PL intensity decay in InAs QDs as a rule attributed to thermal escape of carriers from QDs into the wetting layer or into the GaAs barrier [5-8], as well as to thermally activated capture of excitons by nonradiative defects in the GaAs barrier or at the GaAs/InAs interface [5, 9, 10]. The unusual variations of emission energy and the full width at half maximum (FWHM) of PL bands in the InAs/GaAs self-assembled QDs have been investigated earlier as well [11, 12]. A decrease in the FWHM, together with a red shift of the emission wavelength were explained by the re-localization of carriers between dots caused by their inhomogeneous sizes. A set of theoretical works has been devoted to these questions, which described the carrier dynamics in QD systems using a rate equation model [13-19].

However, it is not still clear the details of exciton capture and thermal escape in high quality QD structures. Two main ways are discussed: a) thermal escape (capture) of carriers (electron and hole) in/from QDs takes place as an exciton or correlated electron-hole pairs [17, 18]; or b) the excitons dissociate and single electrons (holes) thermally escape or capture independently [19-21].

The first mentioned mechanism is the subsequence of the fact that the activation energy of ground state PL thermal decay measured in the regime of strong quenching matches the difference between the GaAs band gap and QD ground state (GS) energy (the sum of barrier heights for electrons and holes) [17-19]. The same effect was earlier revealed in strained InGaAs/GaAs QWs, where the activation energy of PL thermal decay corresponded to the difference between the GS energies of QW and the GaAs barrier, defined as total confinement energy, i.e. the sum of electron and hole potential depths. The main conclusion follows from this fact: excitons or electron-hole pairs are emitted from QWs into the barrier [22].

The motivation for the second mechanism was presented in [19-21]. It was shown in [19] at the InAs/GaAs QD PL investigation under low excitation and high temperature the ground state PL intensity varies quadratically with excitation density. This fact was explained as an evidence of independent occupation of QDs by electrons and holes with the probability which is proportional to the multiplication of their concentrations ($n_e n_p$).

Other evidences for supporting the second approach were shown in [20] at the investigation of cathodoluminescence thermal quenching in InAs/GaAs self-assembled QDs at high-excitation conditions. The significant reductions in the thermal activation energies in the 230–300^{o}K temperature range for the ground (GS) and excited states (ES) are found. It was suggested that excitons dissociate and the thermal reemission of single holes from QD states into the GaAs is responsible for the observed temperature dependence. The same explanation was supposed in [21] at the joint investigation of InAs QD and InGaAs QW PL thermal decays.

In DWELL structures the introduction of surrounding $In_xGa_{1-x}As/GaAs$ QWs changes the QD density, the elastic strain in structures, the height of potential barriers for exciton capture and thermal escape in/from QDs as well as can increase in some cases the density of nonradiative (NR) centres. In these structures the mechanism of PL intensity thermal decay could depend strongly on parameters of DWELL. Improved understanding of the operation and design of InAs/InGaAs QD-based devices could be emanated from studies involving the excitation and temperature dependences of PL in such structures.

Note the highest emission intensity of QDs was achieved in the symmetric wells with the composition of quantum well (QW) capping/buffer layers of $In_{0.15}Ga_{0.85}As/GaAs$ [3]. One of the best methods of manipulating the InAs QD density and sizes inside of QWs related to controlling the QD growth temperatures [3,12-15]. But even for the optimal QD growth parameters and capping/buffer layer compositions, the InAs QD structures are characterized by photoluminescence (PL) inhomogeneity along the wafers [16-19].

The inhomogeneity of InAs QD parameters across the wafer due to the size, chemical composition and stress variations leads to a broadening of emission spectra. This type of problems in QD structures was investigated using scanning PL spectroscopy [23, 26-29], high resolution transmission electron microscopy [30], scanning tunneling microscopy [31], as well as spatially resolved scanning tunneling luminescence [32]. However, in dot-in-a well structures, where the InAs QDs coupled with InGaAs/GaAs QWs, the physical reasons of emission inhomogeneity still have to be discussed. The technology of growth of InAs QD structures has become more reliable recently enabling the systematic studies their physical properties and emission inhomogeneity of QD ensembles.

3. PL spectra of symmetric GaAs/$In_{0.15}Ga_{0.85}As$/GaAs QWs with the different density of InAs QDs

The solid-source molecular beam epitaxy (MBE) in V80H reactor was used to grow the waveguide structures consisting of the layer of InAs self-organized QDs inserted into 12 nm $In_{0.15}Ga_{0.85}As/GaAs$ QWs. The thickness of the buffer $In_{0.15}Ga_{0.85}As$ layer was 2nm, which was grown on the 200.nm GaAs buffer layer and the 2 inch (100) GaAs SI substrate (Fig.1). Then an equivalent coverage of 2.4 monolayers of InAs QDs were confined by the capping (10nm) $In_{0.15}Ga_{0.85}As$ layer and by the 100nm GaAs barrier. Investigated structures are grown under As-stabilized conditions at five different temperatures: 470°C (#1), 490°C (#2), 510°C (#3), 525°C (#4) and 535°C (#5), during the deposition of the InAs active region and InGaAs wells, and at 590-610°C for the rest of layers. All layers were grown with the growth rate of 0.30 ML/s, but for the QD formation the process provides deposition of 2.4 ML with the growth rate of 0.053 ML/s.

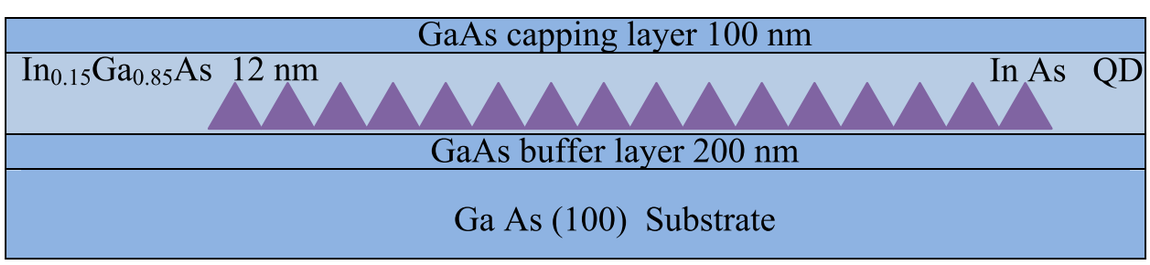

Fig. 1. The schematic design of studied QD structures

For AFM measurement the process of growth was stopped for satelite samples after the formation of QDs. The in-plane density of QDs changed from $1.1x10^{11}$ to $1.3x10^{10}cm^{-2}$ (Table 1) when the temperature increases from 470 up to 535 °C [4, 33]. The samples were mounted in a closed-cycle He cryostat where the temperature is varied in the range of 10 - 300 K. PL spectra were measured under the excitation of the 514.5 nm line of a cw Ar+-laser at an excitation power density form the range of 10-1000 W/cm². The setups used for PL and PL excitation spectroscopies were presented earlier in [5] and [17], respectively.

T_{gr} (°C)	N_{QD} cm^{-2}	D_{QD} nm	h nm	h/D	$S_{QD}^{single} \times 10^{14}$, cm^2	Surface Area of QDs, cm^2
470	1.1×10^{11}	12	6	0.50	113.0	0.124
490	7.0×10^{10}	14	8	0.57	153.9	0.108
510	3.4×10^{10}	18	13	0.72	254.3	0.086
525	1.8×10^{10}	24	11	0.46	452.2	0.081
535	1.3×10^{10}	28	10	0.36	615.4	0.080

Table 1. Average parameters of InAs QDs estimated by AFM [33]

Typical PL spectra of the DWELL structures #2, #3 and #4 measured at different temperatures at the excitation light density of 500 W/cm² are shown in Fig.2. The structures #1 and #2 grown at low temperatures 470 and 490°C are characterized by one PL band only (Fig.2a) with a higher value (Fig.3b) of the full width at half maximum (FWHM). In structures #3, #4 and #5 two PL bands appear due to the recombination of excitons localized at a ground state (GS) and at first excited state (1ES) in QDs (Fig.2b,c).

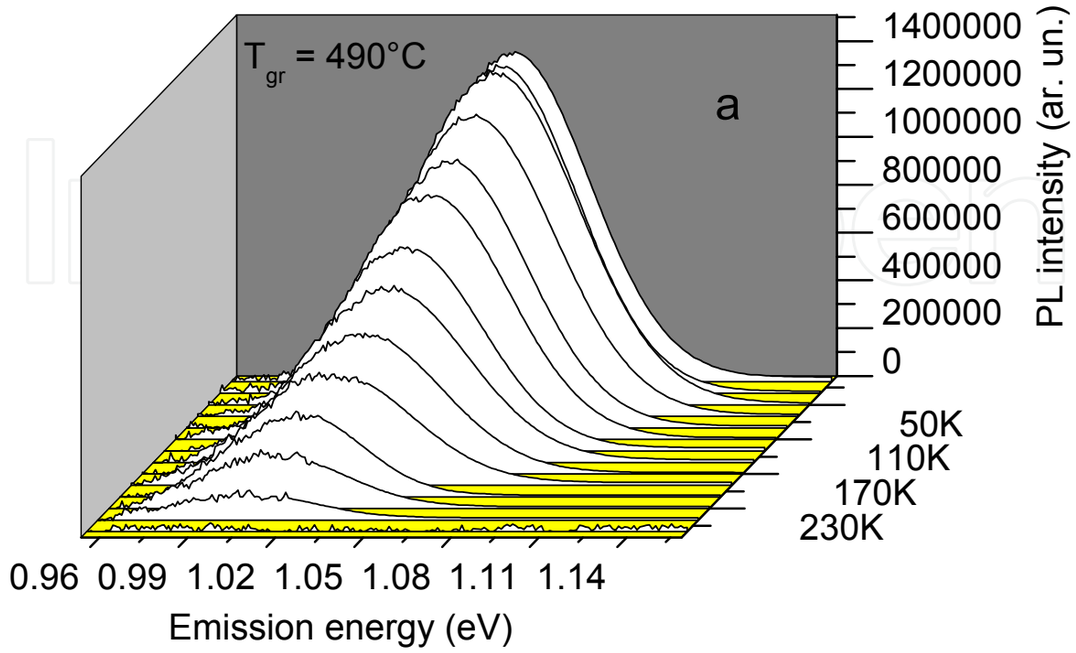

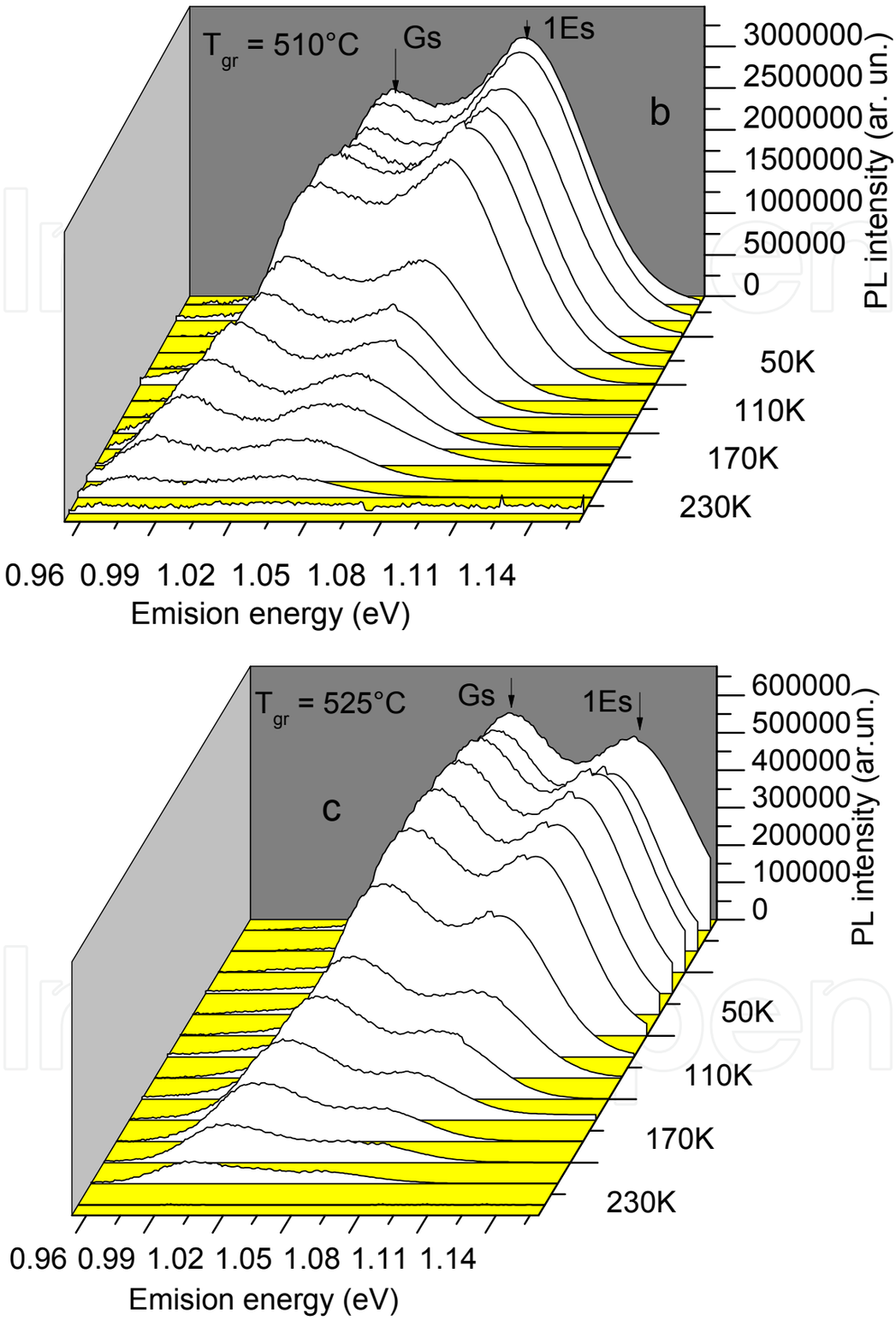

Fig. 2. Typical PL spectra measured at different temperatures for the DWELL structure #2(a), #3(b) and #4(c) at the excitation light density of 500 W/cm².

The density of QDs decreases monotonically with the rise of QD growth temperatures from 470 up to 535 °C (Table 1). Thus the PL intensity diminishing can be expected with reducing a QD density. The QD diameters in studied structures increase monotonically from 12 up to 24-28 nm with the rise of QD growth temperatures from 470 up to 535 °C. Thus it is possible to expect that the PL peak position in QDs has to shift monotonically to low energy.

Fig.3 presents the variation of in plane QD densities, estimated by AFM on satelite samples, as well as the average GS integrated PL intensities and the GS peak FWHM measured at 300K in studied structures.

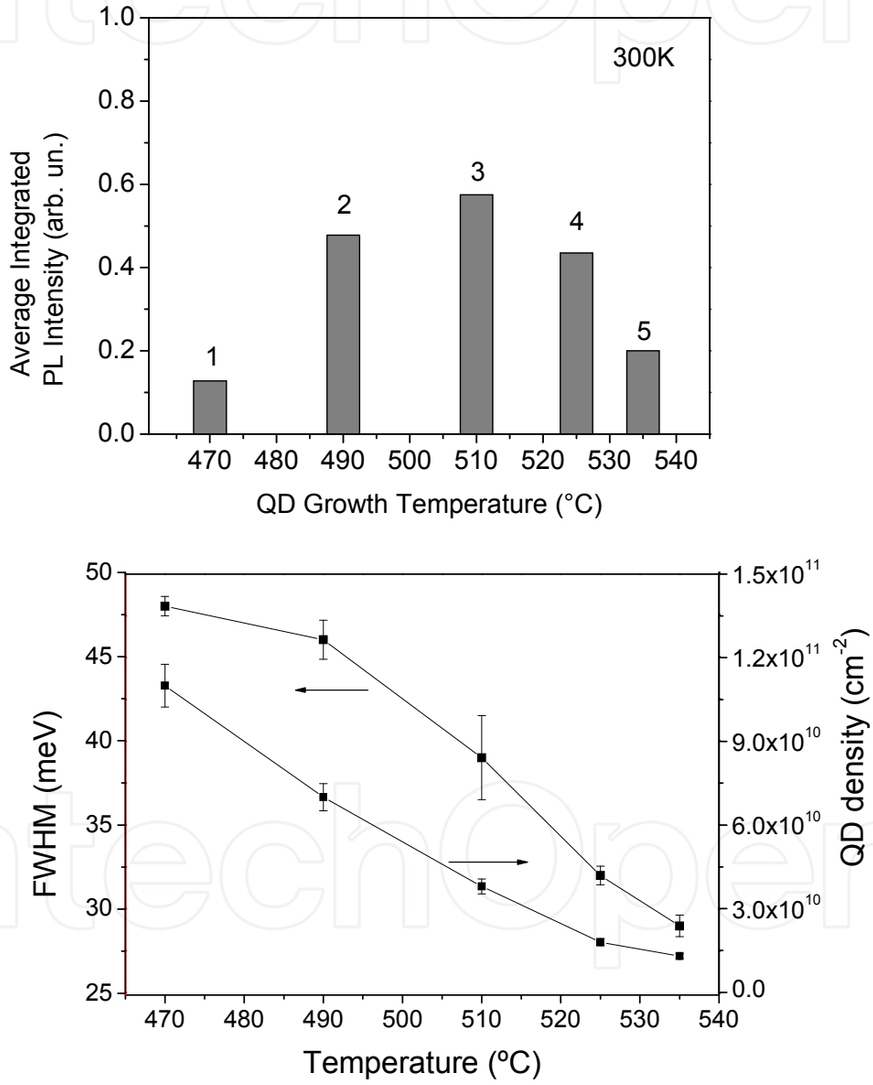

Fig. 3. The average integrated PL intensities measured in DWELLs with QDs grown at different temperatures (a) and the FWHM and QD density in DWELLs with QDs grown at different temperatures (b).

However the PL intensity increases (Fig.3a) and the GS peak shifts to low energy in structures with QDs grown at 490 and 510°C (Fig.2a,b). On the contrary the QD structures

grown at 525 and 535°C are characterized by lower intensities of GS emission (Fig.3a), by smallest FWHM (Fig.3b), and the peak position of GS PL bands shifts into higher energy (Fig.2b,c). Note that lower PL peak energy corresponds to higher PL intensity (Fig.2b and 3a). Thus the variation non monotonous the PL intensity ans peak positions versus QD density (QD growth temperature) has been revealed in studied QD structures.

4. PL excitation spectra of InAs QD structure and PL excitation power dependences

The typical PL excitation spectrum measured at 80K is shown in Fig.4.

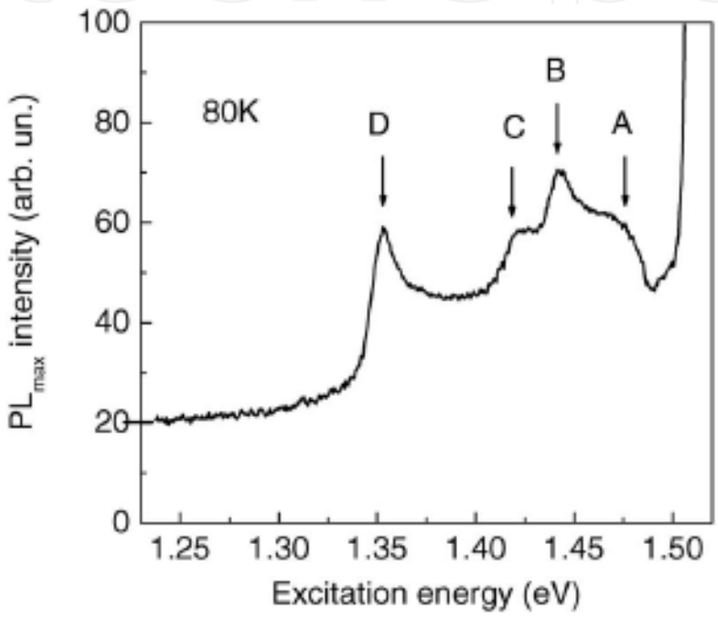

Fig. 4. PL excitation spectrum for the structure #3.

In high excitation energy range the spectrum presents a sharp PL intensity increase due to the fundamental light absorption (at 1.51 eV) in the GaAs barriesr. In the low energy region the PL excitation spectrum can be considered as a superposition of the four absorption bands: A, B, C and D (Fig.4, Table 2).

Optical transitions	GaAs Band gap	peak A	peak B	peak C	peak D	QD-PL	QW-PL
E, eV	1.51	1.46-1.47	1.44	1.42	1.35-1.36	1.06-1.11	1.32-1.33

Table 2. Optical transitions in DWELL structures at 80K

The peak A spectral position (1.46-1.47eV) is close to the GS resonant absorption related to the WL in InAs/GaAs QD structures [17, 24, 25]. Note the authors [25] registrated at 100K in PL excitation spectrum two overlapping maxima (1.45-1.47eV) which were attributed to the photon absorption in the 2D wetting layer between the heavy hole and light hole GS subbands to the GS electronic subband. In studied DWELL structures the GS resonant absorption in the 2 nm buffer $In_{0.15}Ga_{0.85}As$ QW can contribute in other peaks B and C. Thus

both layers (the $In_{0.15}Ga_{0.85}As$ buffer QW and WL) are the same in all studied DWELL structures and can be responsible for the peak A, B and C in the PL excitation spectrum. The spectral position of the lowest energy absorption band (1.35 eV, peak D) is close to one of the PL band (1.31-1.32eV) caused by GS exciton recombination in the capping InGaAs QW (Table 2) [34]. Thus the peak D can be attributed to the GS resonant excitation in the capping $In_{0.15}Ga_{0.85}As$ /GaAs QW (Fig.4).

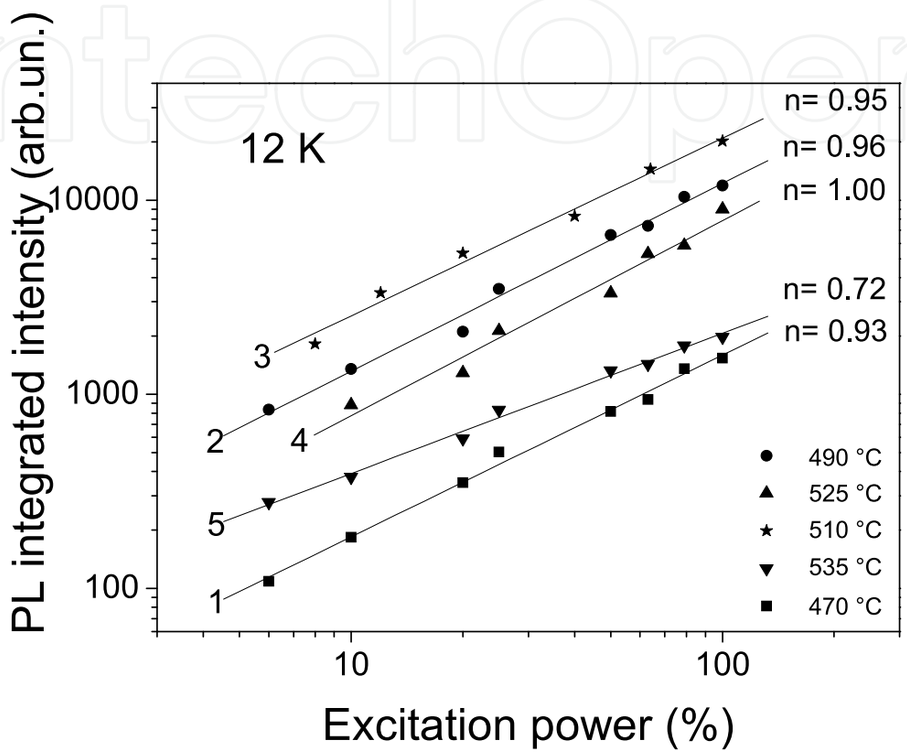

Fig. 5. PL integrated intensity versus excitation power measured for all studied structures

The dependences of integrated PL intensity versus excitation light power, measured at 12K with the aim to avoid the thermal decay process, are presented in Fig.5 for all studied structures. The QD structures #2, #3 and #4 with highest emission intensity are characterized by the linear dependence of the integrated PL intensity (I) versus excitation power ($I \approx P^n$), n=0.95-1.00 (Fig.5). In QD structures with low emission (#1, #5) the integrated PL intensity changes sublineary (n=0.72-0.93) with excitation light power (Fig.5).

5. Emission inhomogeneity along the QD structures

5.1 Scanning PL spectroscopy at 300K

Photoluminescence inhomogeneity of QD ensembles is studied along the scanning line crossed the wafers from the periphery of QD structures to the center. In this case PL spectra were measured at 300 K in a set of points on the QD structures under the excitation by the 804 nm line of a solid state IR laser at an excitation power density of 100 W/cm^2. PL spectra were dispersed by a SPEX 500M spectrometer and recorded by a liquid-nitrogen-cooled Ge detector with a standard lock-in technique.

The inhomogeneity of QD ensemble emission along the line crossed the structures #1 and #2 related mainly to the variation of PL intensity (Fig.6). The integrated PL intensity in the structure #1 is low in comparison with #2, and the variations of PL peak positions are small for both DWELLs (Fig.6): Δhv_m ~0.003 eV (#1) and Δhv_m ~0.010 eV (#2). Thus in QD structures with InAs QDs grown at low temperatures (470-490°C) the less integrated PL intensity (Fig.3a), the high dispersion of QD sizes and, as a result, the larger value of FWHM (Fig.3b) of GS PL bands, but the low dispersion of QD ensemble parameters along the line crossed the structures #1 and #2 have been detected (Fig.6a,b).

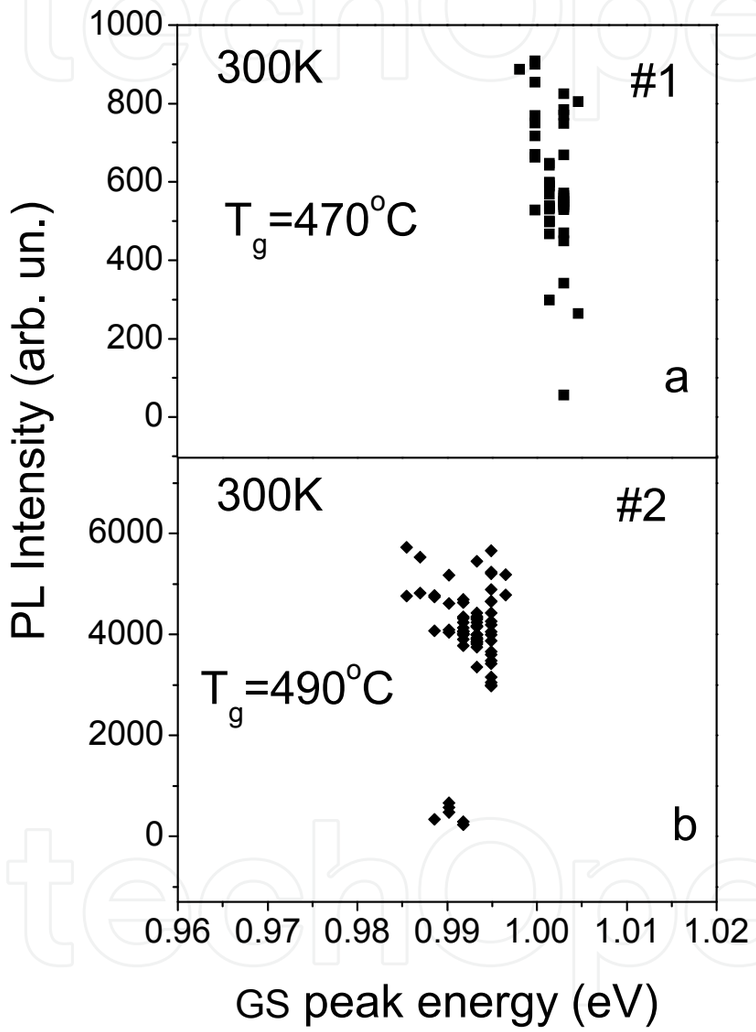

Fig. 6. The PL intensity and GS PL peak positions measured along the line scan from the center of QD structures #1 (a) and #2 (b) to their periphery.

As it follows from fig.7 the decrease of integrated PL intensity, measured along the line from the center to periphery in QD structures #3, #4 and #5, is accompanied by the ''blue'' energy shift of the PL maximum. The FWHM of GS PL bands in the structures #3, #4 and #5 was equal to 35-40 meV (Fig.3b) and it is smaller than those in mentioned above structures #1 and #2. The inhomogeneity of QD ensemble emission along the lines crossed the structures #3, #4 and #5 is characterized by the essential variations of GS peak positions (Fig.7): Δhv_m

~ 0.02 eV(#3), 0.03 eV(#4) and Δhv_m ~0.04 eV(#5), respectively. The integrated PL intensity of QD ensembles in the structure #3 in two- or five-fold higher than in #4 and #5, respectively. Thus in the structures #3, #4 and #5 the low dispersion of QD sizes and, as a result, less values of FWHM, but the essential PL energy shift and the dispersion of QD ensemble parameters along the line crossed the structures have been detected (Fig.7).

The emission inhomogeneity in the QD structures #1 and #2 is related mainly to the change of PL intensity owing the density variations of QDs and/or of nonradiative centers (NR) in QD structures. At the same time the PL peak positions vary negligibly (3-10 meV) testifying that the difference in QD sizes is small. In the structures #3, #4 and #5, as it follows from fig.7, the decrease of PL intensity along the line scan is accompanied by the ''blue'' energy shift of PL maximum. This effect leads at the wafer periphery to shallower QD localized states (i.e. smallest electron and hole binding energy), poorer carrier localization and a higher probability of carrier thermal escape, which reduces the integrated QD PL intensity at 300K.

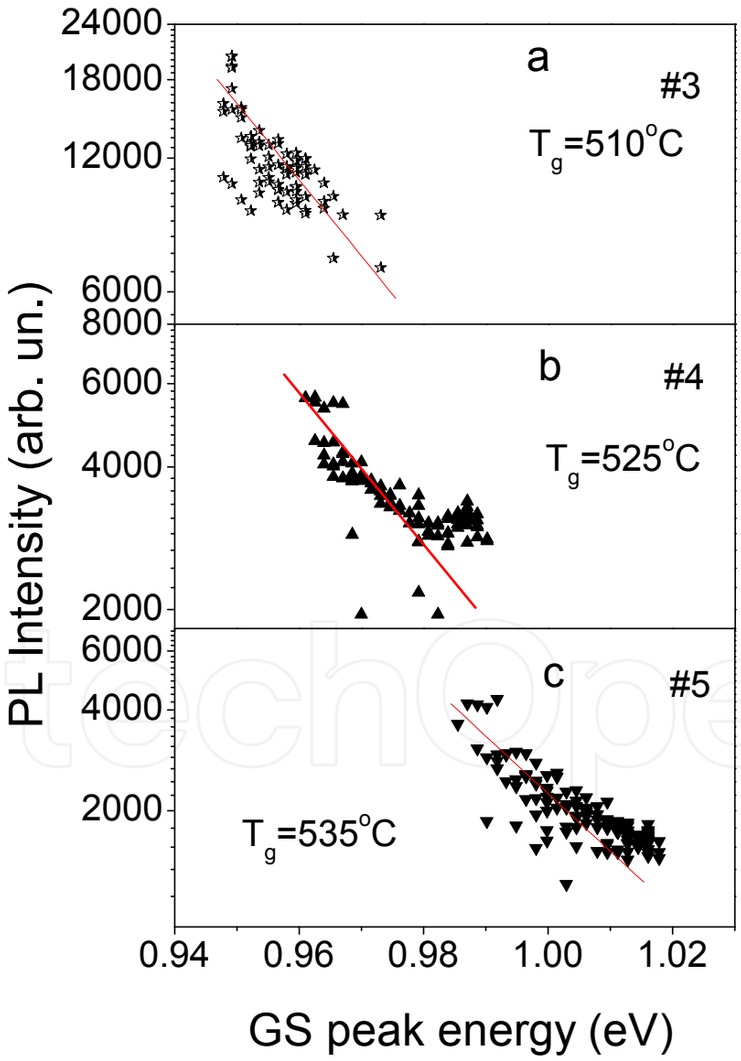

Fig. 7. The PL intensity and GS PL peak positions measured along the line scan from the center of QD structures #3 (a), #4 (b) and #5 (c) to their periphery.

5.2 Analyses of PL inhomogenouty reasons in studied QD structures at 300K

The ground state PL intensity (I_{PL}) of InAs/InGaAs QDs is directly proportional to internal quantum efficiency η which can be presented as: $\eta = \frac{\varpi_R}{\varpi_R + \varpi_{NR}}$. For QD emission the radiative recombination rate is [35]: $\varpi_R = \sum_{i=1}^{N_D} \frac{f_i^e f_i^p}{\tau_R}$, where f_i^e and f_i^p are the occupation probabilities for electrons and holes at ground state levels given by the Fermi-Dirac distribution functions, f^e, f^p=(exp[$(E_{n,p} - \mu_{n,p})/kT$]+1]$^{-1}$, where $\mu_{n,p}$ are the quasi-Fermi-levels for the conduction and valence bands, respectively, measured from the QD band edges, $E_{n,p}$ are the quantized energy levels of an electron and a hole in th conduction and valence bands of a QD, measured from the QD band edges, N_D is QD density and τ_R is electron–hole radiative recombination time in the QD [36]. At low excitation light intensity (100 W/cm^2), used during GS PL scanning, which is well below the GS saturation intensity, we can present the occupation probabilities using Maxwell -Boltzmann distribution functions f^e, f^p=exp($-E_{n,p}$+ $\mu_{n,p}$ /kT). Taking into account that excitation light power is not changed during GS PL scanning experiment, we can assume that $\mu_{n,p}$ are constant along the scanning line and the PL intensity variation occurs due to parameters $E_{n,p}$ only [35]. Thus $f^e \approx \exp \frac{E_{loc}^e}{kT}$ and $f^p \approx \exp \frac{E_{loc}^p}{kT}$, where E_{loc}^p and E_{loc}^e are the binding energy of electron and hole on GS levels in a QD. In this case for GS emission intensity at room temperature is possible to write:

$$I_{PL} \approx \tau_R^{-1} \approx \sum_1^N \frac{1}{\tau_{RQD}} \exp\left(\frac{E_{loc}^e + E_{loc}^p}{kT}\right) \approx \sum_1^N \frac{1}{\tau_{RQD}} \exp\left(\frac{E_{GS}^{InGaAs} - E_{GS}^{QD}}{kT}\right) \approx \exp \frac{-E_{GS}^{QD}}{kT} \qquad (1)$$

where E_{GS}^{InGaAs} is energy gap between electron and hole quantized levels in narrow-gap $In_{0.15}Ga_{0.85}As$ layer and E_{GS}^{QD} is energy gap between electron and hole quantized levels in QD. Finally the GS PL optical transition energy ($hv_{\max}^{GS}$) is the difference between E_{GS}^{QD} and exciton binding energy E_{bin}^{ex} in QDs. Exciton binding energies were computed as the function of QD size using 8-band **k·p** approach and are estimated as 22 meV for QDs with the base size 14 nm [37]. Thus the E_{bin}^{ex} value is small in comparison with GS PL optical transition energy ($hv_{\max}^{GS}$) equal to 1.06-1.11 eV. If the InGaAs composition is the same in any points of the capping/buffer layers, the linear dependence of GS PL intensity versus PL peak positions in QD ensembles in semi-logarithmic plot follows from Eq.1 (Fig.7). At the same time the slope of this linear dependence is proportional to kT. The fitting procedure was applied to the analysis of PL intensity data presented in Fig.7 and the slopes of these three lines were estimated as ~25 meV that is exactly the value of kT at 300K. Thus the analysis of linear dependence in Fig.7 testifies that the variation of GS PL intensity in the QD ensemble along the line scan in the structures #3, #4 and #5 is owing to the QD size variation – its decreasing from the wafer center to the periphery [38]. The last effect can be connected with temperature inhomogeneity along the wafer at the QD growth process.

6. Temperature dependences of PL integrated intensities and peak positions

Two reasons can explain the variation non monotonically of PL peak positions and the PL intensity in studied QD structures (Fig.2 and 3a): (i) the change of QD composition due to the Ga/In inter diffusion between the InAs QDs and capping/buffer $In_{0.15}$ $Ga_{0.85}As$ QW layers or (ii) the different levels of elastic strains in QD structures due to the difference in QD densities and sizes. To distinguish these two reasons PL spectra at different temperatures in the range 12-300 K have been studied. The temperature dependences of integrated PL intensities and peak positions of GS PL bands for the structures #1, #3, #5 are shown in Fig.8.

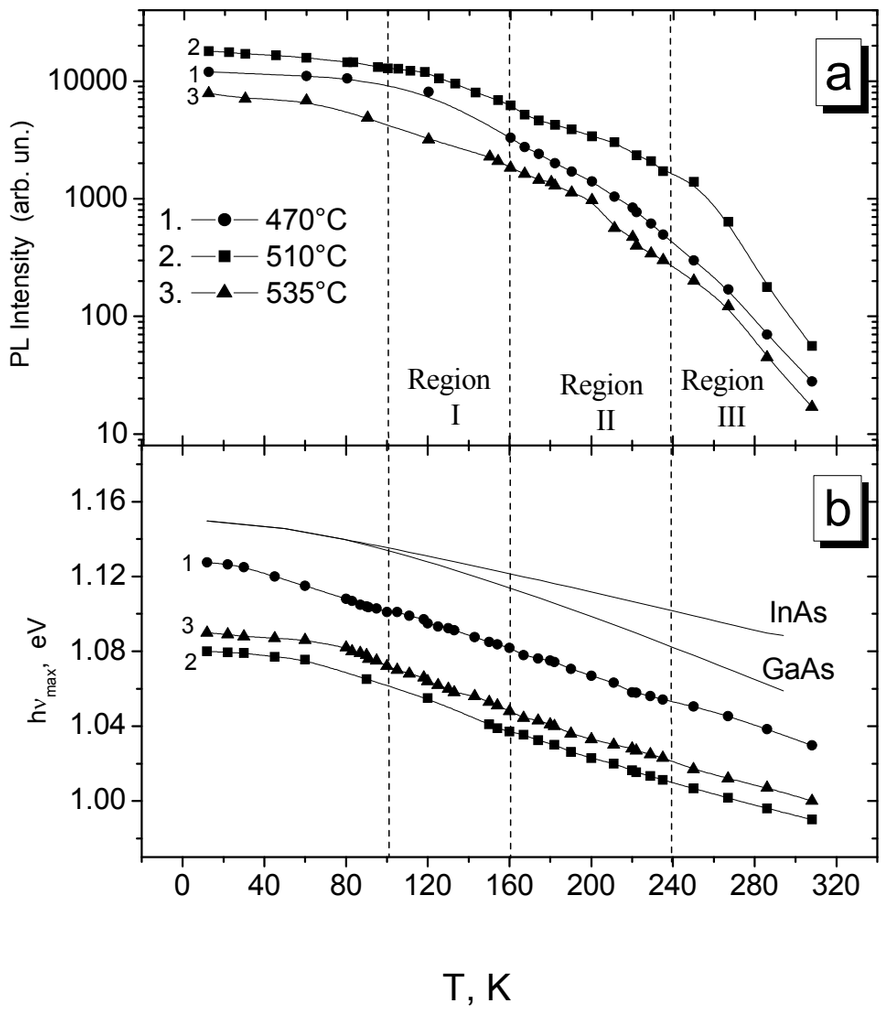

Fig. 8. Temperature dependencies of GS integrated PL intensities (a) and GS peak positions (b) measured for the structures #1, #3 and #5. Lines present the fitting results.

The process of PL thermal decay starts at 80-120 K and it is characterized by different rates in the ranges T=100-180 K, T=180-250 K and T=250-300 K. At low temperatures up to 100 K the integrated PL intensity does not change, but the energy of GS peak decreases. The process of PL intensity decay starts at 100-120K in high quility structures #2, #3 and #4, but in structures of low quality (#1, #5) this process appears at 80-90K.

7. The analysis of Ga/In interdiffusion in QD structures with different density of InAs QDs

Fig. 9 presents the variation of PL peak positions versus temperature in studied structures. PL peaks shift to low energy with increasing temperature due to the optical gap shrinkage. The lines in Fig.9 are the fitting results analyzed on the base of Varshni relation that presents the energy gap variation with temperature as [39]:

$$E(T)=\mathrm{E_o}-\frac{aT^2}{T+b} \tag{2}$$

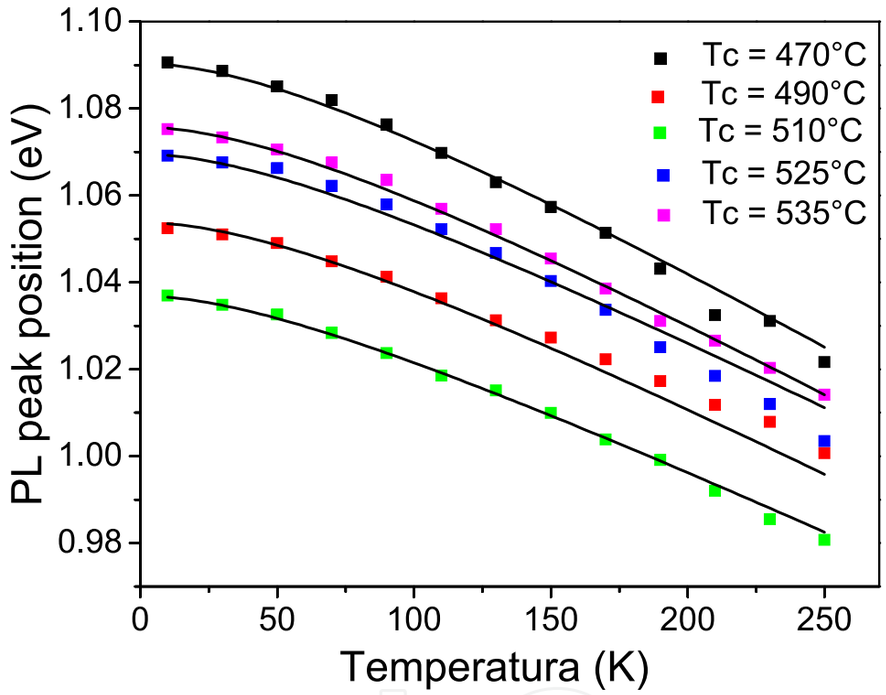

Fig. 9. The variation of PL peak positions versus temperature. The lines present the Varshni fitting results: 1- #1, 2- #2, 3- #3, 4-#4 and 5 - #5.

The comparison of fitting parameters with the variation of energy band gap versus temperature in the bulk InAs and GaAs crystals (Table 3) has revealed that in studied QD structures the fitting parameter "a" and 'b' in the temperature range 12-250 K are very close to their values for the bulk InAs crystal only in the structures #2 and #3. But in other QD structures the fitting parameter "a" and 'b' are different a little bit from the values in the bulk InAs crystal (Table 3). The last fact testifies that the process of Ga/In inter diffusion takes place in these QD structures [33,42-44]. Note that the process of Ga/In inter diffusion in studied structures passes non monotonically versus QD growth temperatures. It means that not only temperature but some other factors discussed below are essential as well.

	E_0	A	b
Structure numbers	eV	meV/ ^oK	^oK
#1	1.082	0.355	110
#2	1.089	0.346	98
#3	1.010	0.300	95
#4	1.049	0.330	110
#5	1.079	0.335	130
InAs [40]	0.415	0.276	93
GaAs [41]	1.519	0.540	204

Table 3. The Varshni fitting parameters

8. Model for the dependence of PL integrated intensity versus temperature

An analysis of the thermal behavior of QD luminescence indicates that excitons are the dominant electronic particles. Thus to modeling the dependence of the ground state PL intensity versus temperature the simple assumption is applied: the carriers are considered to behave as excitons or correlated electron-hole pairs. This assumption is a common feature of most exiting models [15-18]. The motivation of the choosing this approach in this paper will be clear from presented esperimental results as well.

For InAs/InGaAs structures, the two-stage processes of exciton capture and thermal escape in/from QDs have been considered [17, 33]. These processes in QD structures can occur not only through the wetting layer (WL) states, as was proposed earlier [16, 18], but also through the capping/buffer InGaAs QW layers [17, 33]. However in [17] the localization of nonradiative defects was considered in GaAs barrier mainly. In present model two types of nonradiative defects: in the GaAs barrier (NR1) and in the capping/buffer $In_{0.15}Ga_{0.85}As$ QWs (NR2) are taken into account [33]. To simplify the rate equations, one intermediate level, referred as QW, will be considered in the model.

It is supposed that photo-generated excitons are created in GaAs barrier and in $In_{0.15}Ga_{0.85}As$ QWs with generation rates G_{GaAs} and G_{InGaAs}, respectively. The exciton recombination takes place in the GaAs barrier, InGaAs QWs and in InAs QDs. In this model all QDs in an ensamble are assumed to be identical with the same properties and the process of carrier thermal redistribution between QDs is inessential. This is supported by the experimental fact that the FWHM of the ground state PL band is measured to be constant in the temperature range of 10-300K. The system of rate equations for exciton concentrations in the GaAs barrier (C_o,), QWs (C_1) and QDs (C_2) can be written as:

$$\frac{dC_0}{dt} = G_{GaAs} - \omega_{QW} C_0 N_{QW} + \omega_{QW} C_1 N_{GaAs} \exp\left(-\frac{\Delta E^{GaAs-QW}}{kT}\right) - \frac{C_0}{\tau_{NR1}} \tag{3}$$

$$\frac{dC_1}{dt} = G_{InGaAs} + \omega_{QW} C_0 N_{QW} - \omega_{QW} C_1 N_{GaAs} \exp\left(-\frac{\Delta E^{GaAs-QW}}{kT}\right) - \omega_{QD} C_1 N_{QD} + \\ + \omega_{QD} C_2 N_{QW} \exp\left(-\frac{\Delta E^{QW-QD}}{kT}\right) - \frac{C_1}{\tau_{RQW}} - \frac{C_1}{\tau_{NR2}} \tag{4}$$

$$\frac{dC_2}{dt} = \omega_{QD} C_1 N_{QD} - \omega_{QD} C_2 N_{QW} \exp\left(-\frac{\Delta E^{QW-QD}}{kT}\right) - \frac{C_2}{\tau_{RQD}} \tag{5}$$

Here $\varpi_{QW} N_{QW} = \tau_{QW}^{-1}$ and $\varpi_{QD} N_{QD} = \tau_{QD}^{-1}$ are exciton thermalization (capture) rates from the GaAs barrier into QWs and from QWs into QDs, respectively, N_{QD}, N_{QW}, N_{GaAs} is the density of states in QDs, QWs and in the GaAs barrier, ϖ_{QW}, ϖ_{QD} are the exciton capture coefficients into QWs and QDs, τ_{RQW}^{-1}, τ_{RQD}^{-1}, τ_{NR1}^{-1} and τ_{NR2}^{-1} are the radiative exciton recombination rates in QWs and QDs as well as the nonradiative recombination rates in the GaAs barrier and in QWs, respectively. The values $E^{GaAs-QW}$, E^{QW-QD}, $E^{GaAs-QD}$ are the energy differences between: (i) the GaAs band gap and the GS energy in QWs, (ii) the GS energy in QWs and in QDs, (iii) the GaAs band gap and the GS energy in QDs, respectively.

The temperature dependence of the exciton escape rates from QWs and QDs is taking into account, but temperature dependences of other parameters (trapping and recombination coefficients, density of states, exciton thermalization rates) are neglected. This is motivated by simplifying the calculation process and by minimization of the number of parameters samulteniously with significant progress in understanding the experimental results. Several comments deal with the experimental base for such simplifications are discussed below.

In presented model the variation of the GS PL intensity (I(T)) in QDs versus temperature in the stationary state can be described by the formula:

$$I(T) = \frac{G_{InGaAs} + G_{GaAs}\left(1 - \frac{\tau_{NR1}^{-1}}{\tau_{QW}^{-1} + \tau_{NR1}^{-1}}\right)}{1 + \frac{\tau_{RQW}^{-1} + \tau_{NR2}^{-1}}{\tau_{QD}^{-1}} + \frac{\tau_{NR1}^{-1}\tau_{QW}^{-1} N_{GaAs}}{\tau_{QD}^{-1}\left(\tau_{QW}^{-1} + \tau_{NR1}^{-1}\right) N_{QW}} \exp\left(-\frac{\Delta E^{GaAs-QW}}{kT}\right) + \frac{\left(\tau_{RQW}^{-1} + \tau_{NR2}^{-1}\right) N_{QW}}{\tau_{RQD}^{-1} N_{QD}} \exp\left(-\frac{\Delta E^{QW-QD}}{kT}\right) + \frac{\tau_{QW}^{-1}\tau_{NR1}^{-1} N_{GaAs}}{\tau_{RQD}^{-1}\left(\tau_{QW}^{-1} + \tau_{NR1}^{-1}\right) N_{QD}} \exp\left(-\frac{\Delta E^{GaAs-QD}}{kT}\right)} \tag{6}$$

Here the radiative lifetime in QDs (τ_{RQD}) is assumed to be constant with T as expected theoretically for strong confinement in three dimensions [15-18]. The radiative recombination rate in InGaAS/GaAs QWs (τ_{RQW}), as was shown in [22], is controled mainly by nonradiative recombination processes at the T≥100K. The dependence of the nonradiative rate in InGaAs/GaAs QWs was investigated as well in [22]. Its value in QWs, as a rule, increases at low temperatures and saturates at 120-150K at a constant value depending on the quality of the structure. As result it is possible to neglect by temperature dependences of the parameters: τ_{RQW}^{-1}, τ_{NR1}^{-1} and τ_{NR2}^{-1} at the T≥120-150K.

The exciton thermalization (capture) rates from the GaAs barrier into a QW τ_{QW}^{-1} and from a QW into QDs, τ_{QD}^{-1}, are the multiphonon-assisted processes deal with the scattering via multiple longitudinal optical phonon (LO) emission [41-43]. The values τ_{QW}^{-1} and τ_{QD}^{-1} have to increase versus temperature due to the enlargement of the phonon number. However, it was shown in [42] that the PL rise time in a QW (dependent on the exciton capture rate into QWs, τ_{QW}^{-1}) for all temperatures from the range 50-300K is the same about 1-2 ps.

The dominant multiphonon capture mechanism and the InGaAs/GaAs QD capture time τ_{QD}^{-1} decreasing with temperature were confirmed experimentally in time-resolved

experiments [45-47]. It was shown using the investigation of the PL rise time for the GS in QDs that its value decreases: from 6.5ps to 3.5ps upon increathing the temperature from 4 to 300K [45], or from 15ps to 7ps at the temperature rise from 50 to 300K [46]. Thus nearly two-fold decreasing of the exciton capture time into QDs is revealed experimentally versus temperature. It is essential that the temperature dependence of the exciton escape rates from QWs and from QDs obviously much stronger and it is taking into account in the model.

9. Discussion of PL integrated intensity dependences versus temperature

It is clear from the formula (6), that in high quality QD structures (#2, #3 and #4) with low concentrations of the NR1 and NR2 centres the PL intensity I(T) is linearly dependent on excitation power (or generation rates, G_{InGaAs}, G_{GaAs}), as it is demonstrated in Fig.5. In low quality QD structures (#1 and #5) photo-generated excitons recombine partially via NR1 and NR2 centres and W (T) changes Sublineary versus power (Fig.5).

The analysis of PL temperature dependences is resonable to provide for the temeparture ranges I – III separately (Fig.8). At low temperature (< 100K) the processes of exciton thermal escape from a QW into the GaAs barrier and from QDs into a QW are not essential, and the PL intensity I (T) does not change (Fig. 8).

In the temperature ranges I00-300K following the model the activation energy of PL thermal decay has correspond to the values $E^{GaAs-QW}, E^{QW-QD}, E^{GaAs-QD}$. To quantitative determination of activation energies the $\{I_{max}/I(T) - 1\}$ dependences for the GS and ES PL bands were plotted versus temperature in Arrhenius plots (Fig.10). Three distinct linear regions (I-III) with the corresponding activation energies Ea (I), Ea (II) and E_a(III) are observed for different temperatures (Fig.10).

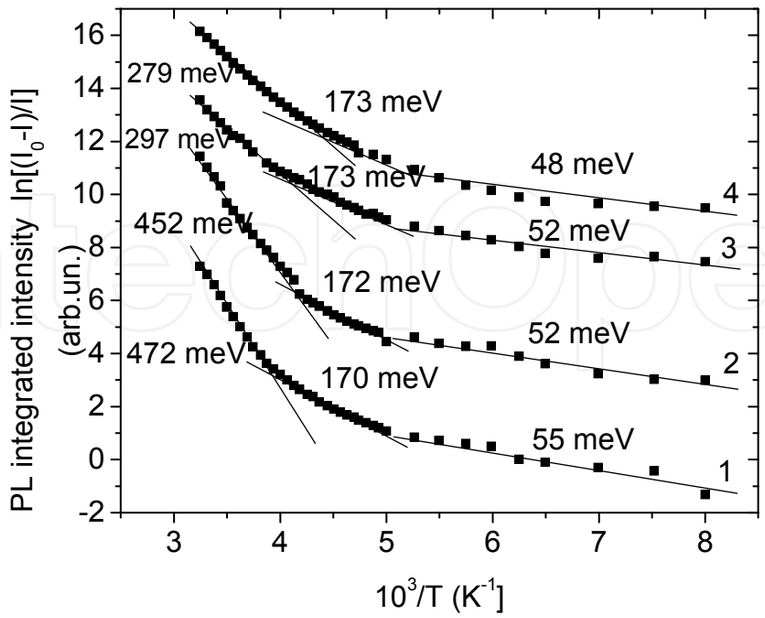

Fig. 10. Arrhenius plots for the thermal decay of the GS integrated PL intensity measured at the power density of 500W/cm² for the structures #3 (1), #2 (2), #1 (3) and #5 (4).

In the range I (100-180K) the activation energy (Ea (I) = 48-55 meV) of PL decay measured at low excitation power for GS PL bands (Fig.10) is very close to the energy difference between the GaAs band gap and the GS energy of the WL and/or the buffer InGaAs QW layer (peak A, B, C in Fig.4, Table 2). It can be supposed that thermal quenching of the GS PL intensity in the temperature range I is due to decreasing an exciton flow to QDs caused by thermal escape of excitons from the WL (or buffer InGaAs QW) into the GaAs barrier where they are lost through subsequent nonradiative recombination. If the above mentioned mechanism takes place in QD structures the same activation energy ($E^{GaAs-QW}$) has to be detected in the range I for thermal decay of PL bands connected with the GS and ES of QDs, as well as for the QW PL band. Actually the results presented in Fig.11 testify that in the range I thermal decay of PL bands deal with the GS, four ES in QDs, as well as with a QW is characterized by the same activation energy from the range 48-53meV.

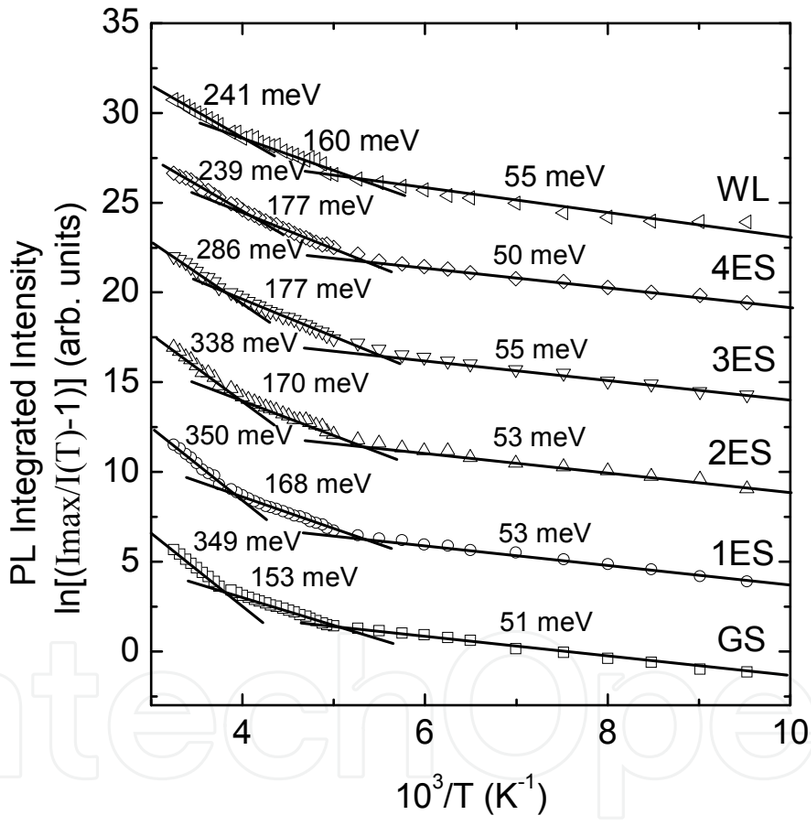

Fig. 11. Arrhenius plots for the thermal decay of the integrated PL intensity measured at the power density of 1000W/cm² for the QD structures #3

In the temperature range II (180-250K) the activation energy (Ea (II) = 170-173 meV) of PL decay for GS bands (Fig.10 and 11) is very close to the energy difference between the GaAs band gap and the GS energy for the capping $In_{0.15}Ga_{0.85}As$ QW (peak D, Fig.4, Table 2). Thus the process of thermal decay of the QD PL intensity in the range II can be attributed to diminishing of an exciton flow to QDs caused by thermal escape of excitons from the capping $In_{0.15}Ga_{0.85}As$ QW into the GaAs barrier. This explanation is confirmed as well by

the thermal quenching of PL bands deal with the GS and 1ES-4ES in QDs, and with the capping QW. All PL bands in the range II demonstrate the activation energy from the range of 153-177 meV (Fig.11).

At high temperatures, stage III (250-300K), the activation energy of PL thermal decay depends on the quality of DWELL structures (Fig.10). As one follows from the formula (6) the activation energy of PL thermal decay will be close to the value $\Delta E^{GaAs-QD}$ if the follows two relations are correct:

$$\frac{\left(\tau_{RQW}^{-1}+\tau_{NR2}^{-1}\right)N_{QW}}{\tau_{RQD}^{-1}N_{QD}}\exp\left(-\frac{\Delta E^{QW-QD}}{kT}\right) << \frac{\tau_{QW}^{-1}\tau_{NR1}^{-1}N_{GaAs}}{\tau_{RQD}^{-1}\left(\tau_{QW}^{-1}+\tau_{NR1}^{-1}\right)N_{QD}}\exp\left(-\frac{\Delta E^{GaAs-QD}}{kT}\right) \quad (7)$$

or after the simplification of the (7):

$$(\tau_{RQW}^{-1}+\tau_{NR2}^{-1})N_{QW}\ \exp\left(-\frac{E_{GS}{}^{QW}}{kT}\right) << \frac{\tau_{QW}^{-1}\tau_{NR1}^{-1}N_{GaAs}}{\left(\tau_{QW}^{-1}+\tau_{NR1}^{-1}\right)}\ \exp\left(-\frac{E_{g}{}^{GaAs}}{kT}\right) \quad (8)$$

It means that if the concentration of nonradiative defects in QWs (NR2) is low the activation energy of PL thermal decay for the GS PL band in QDs will approach to the value $\Delta E^{GaAs-QD}$. Actually for the high quality structures (#2, #3) the activation energies (452 and 472 meV) in the range III (Fig.10) are close to the $\Delta E^{GaAs-QD}$. Note this value is the sum of the barrier energy for electrons and holes in QDs. It testifies that just excitons thermally escape in the range III from QDs into the GaAs barrier with subsequent NR recombination. In the case of measurement at the high excittaion power (Fig.11) the decrease of activation energy for GS thermal decay deals with exciton re-localization from the ES to the GS of other QDs which slow down the process of GS thermal quenching.

In low efficient QD structures (#1, #5) the process of GS PL thermal decay is characterized by smaller activation energies, 279 and 297 meV (Fig.10). For these structures it is natural to supose the high concentration of the NR2 centers in InGaAs QWs. It means the conditions (7) and (8) do not satisfy. As one follows from the formula (6) in this case the activation energy of GS PL thermal decay will approach to the value ΔE^{QW-QD}.

Note that obtained experimental results do not present an evidence for the exciton thermal dissociation in QWs or in QDs at high temperatures with subsiquent re-localization, thermal escape or tunneling of separated electrons or holes. If the process of exciton thermal dissociation is realized the activation energy of GS PL thermal decay should be smaller and comparative with the value of barriers for electrons or holes in the QD structures that was not observed.

10. Fitting of the data of PL integrated intensity thermal decay

The fitting procedure was applied to the experimental curves for thermal decay of integrated PL intensities presented in Fig.8. As it follows from Eq.6 the integrated PL intensity thermal decay can be simulated as:

$$I = \frac{I_0}{1 + K_1 \exp(-E_1/kT) + K_2 \exp(-E_2/kT) + K_3 \exp(-E_3/kT)} \quad (9)$$

The values I_o and the activation energies E_1, E_2 and E_3 for different temperature ranges (I-III) were taken from the experimental results presented in Fig.10 (Table 4). Parameters K_1, K_2 and K_3 have been obtained from the numerical simulation procedure (Table 4) [48,49]. As it follows from Eq.6 the coefficients K_1 and K_3 related to the exciton nonradiative recombination rate (τ_{NR1}^{-1}) in the GaAs barrier, but the coefficient K_2 depends on the exciton nonradiative recombination rate (τ_{NR2}^{-1}) in InGaAs QWs. Numerical simulation results presented in Table 4 have shown that the coefficients K_1 and K_3 related to the exciton nonradiative recombination rate (τ_{NR1}^{-1}) in the GaAs barrier of the structure #3 are less in comparison with those in #1 and #5 [48-50]. Simultaneously the coefficient K_2 related to the exciton nonradiative recombination rate (τ_{NR2}^{-1}) in InGaAs QWs for the structure #3 is one order smaller than in #1 and #5. These facts are the reason of fast PL thermal decay and lower integrated PL intensities in structures #1 and #5 in comparison with the structure #3.

Structure	I_o	E_1 meV	E_2 meV	E_3 meV	K_1	K_2	K_3
#1	$1.1\ 10^4$	53	174	451	100	$2.0\ 10^5$	$6.7\ 10^9$
#3	$1.7\ 10^4$	52	175	452	85	$2.3\ 10^4$	$6.0\ 10^9$
#5	$8.9\ 10^3$	54	173	450	100	$2.3\ 10^5$	10^9

Table 4. Fitting parameters estimated from the PL thermal decay

Thus, it is shown that the excitonic nature of carriers is important for the processes of capture and thermal escape in/from QDs in DWELL structures. At low temperatures the GS and ES PL thermal decays are attributed to the reduction of exciton flow into the QDs due to the exciton thermal escape from the WL or InGaAs buffer layers (100–180 K) or from the GS of capping $In_{0.15}$ $Ga_{0.85}$ As layers (180–250 K) into the GaAs barrier with subsequent NR recombination. At high temperatures (250–300 K) the activation energy of PL thermal decay depends on the QD density and the quality of DWELL structures. In DWELL structures with high emission (#2,# 3, and #4) the activation energy matches the energy difference between the GaAs band gap and the GS level of QDs. In structures with weak emission (#1 and #5) the activation energy is close to the energy difference between the GS level of QDs and the GS energy level in InGaAs/GaAs QWs. The reasons of DWELL quality variation versus QD density are discussed below.

11. X ray diffraction study in InAs QD structures with the different densities of QDs

It is important to discuss the reasons of the quality change in studied QD structures with different InAs QD densities. The application of the capping/buffer In_xGa_{1-x} As layers in the QD structure has been demonstrated as an effective means to the QD density increase

[3], to tune the GS PL transition to the 1.3 μm spectral region [3,17, 51] and to narrow a PL line width [52]. However, the structural and electronic properties of InAs QDs coupled with In_xGa_{1-x} As/GaAs QWs are still understood partially. It is generally supposed that this type of growth provides the potential to strain engineering of structural and electronic properties due to efficient strain relaxation altering the electronic potential of capped QDs [51, 53]. Additionally the In_xGa_{1-x} As layer reduces the inhomogeneous surface stress enhancing the ability to grow a multitude of identical uncorrelated QD layers [51]. The majority of publications considered the stress variation in the vicinity of QDs or ordered arrays of QDs [52-58].

To investigate the strain levels in QD structures the X ray diffraction (XRD) has been studied. The XRD experiments were made using the XRD equipment model of D-8 advanced (Bruker Co.) with $K_{\alpha 1}$ line from the Cu source (λ=1.5406Å). Figure 12 present the superposition of XRD peaks related to the diffraction of $K_{\alpha 1}$ and $K_{\alpha 2}$ lines of Cu source from the (400) crystal planes of the cubic GaAs substrate and GaAs layers in studied InGaAs/GaAs QWs [59.60].

	(400)				(200)		
Material	$2\theta_1$ (degree) $K_{\alpha 1}$	$2\theta_1$ (degree) K_{β}	d_1, A	$2\theta_2$ (degree) $K_{\alpha 2}$	$2\theta_1$ (degree) $K_{\alpha 1}$	d_2, A	$2\theta_3$ (degree) $K_{\alpha 2}$
GaAs Bulk	66.044	59.0165	1.414	66.225	31.63	2.828	31.71

Table 5. Values of 2θ angles for the diffraction of $K_{\alpha 1}$, $K_{\alpha 2}$ and K_{β} X-ray beams of Cu source from the (400) and (200) cubic GaAs crystal planes [61].

As one can see the peaks (66.05° and 66.24°) related to the diffraction of $K_{\alpha 1}$ and $K_{\alpha 2}$ lines from the (400) crystal planes in GaAs QW structures #2, #3 and #4 with QDs grown at 490-525 °C locate very close to corresponding XRD peaks (66.044° and 66.225° [61]) of the bulk cubic GaAs (Fig.12, Table 5). The last fact testifies that the level of elastic strain in InGaAs/GaAs QWs of #2, #3, #4 is minimum. In contrary in the structures with QDs grown at 470 and 535 °C the corresponding XRD peaks shift to 66.10° and 66.29° (Fig.12) testifying the higher levels of compressive strains in InGaAs/GaAs QWs of these structures.

Figure 13 presents the additional confirmation of conclusions mentioned above. It shows the superposition of XRD peaks related to the diffraction of K_{β} line from the same (400) crystal planes of cubic GaAs substrate and of GaAs layers in InGaAs/GaAs QWs. As one can see the peaks related to the K_{β} line diffraction from the (400) crystal plan of GaAs layers in DWELLs with QDs grown at 490-525 °C (59.036-59.042°) locate close to the corresponding XRD peak in the bulk GaAs (Table 5, Fig.12) for the same (400) crystal plane. Thus the level of elastic strain in these DWELLs is minimum. In DWELLs with QDs grown at 470 and 535 °C the corresponding XRD peaks shift to 59.08° testifing the higher level of compresive strain. Note that the partial relaxation of elastic strain can stimulate the creation of nonradiative recombination centers and due to this decreasing the PL intensity in the structures with QDs grown at 470 and 535 °C.

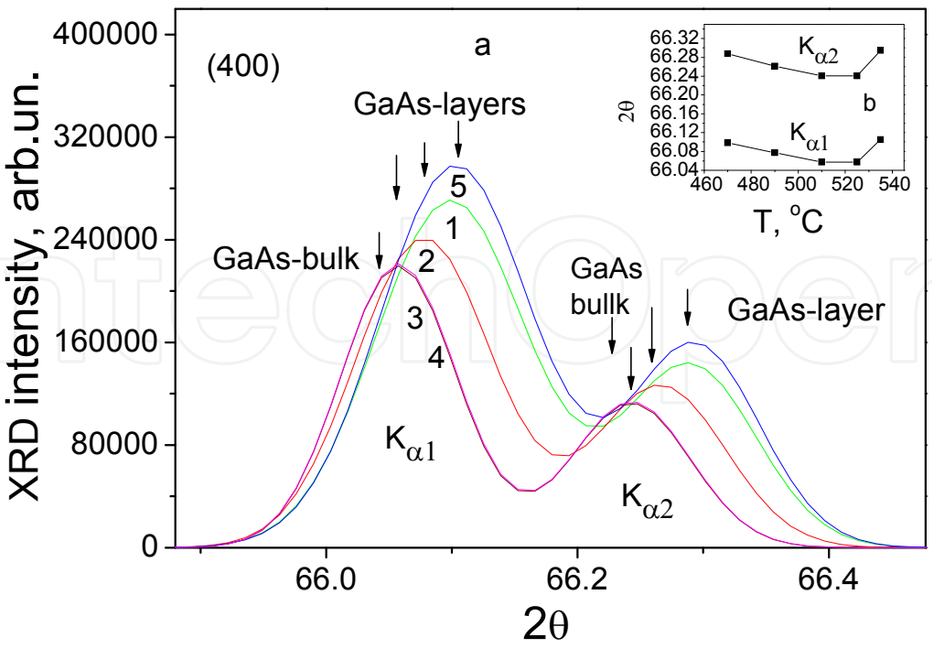

Fig. 12. XRD peaks related to the diffraction of $K_{\alpha 1}$ and $K_{\alpha 2}$ lines on (400) cubic GaAs crystal plane for the structures with QDs grown at 470 (1), 490 (2), 510 (3), 525(4) and 535 °C (5).

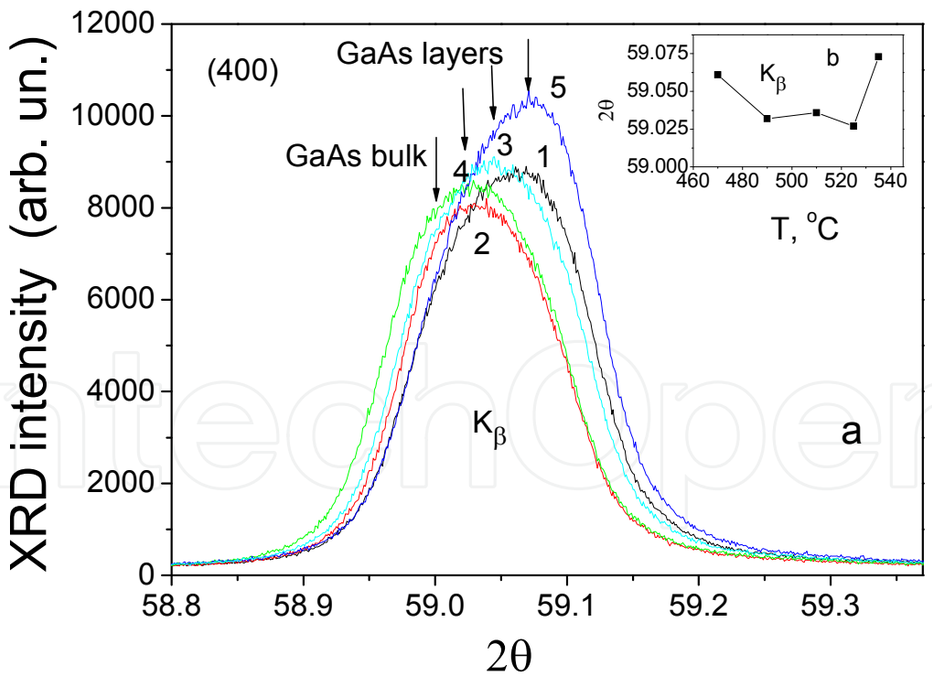

Fig. 13. XRD peaks related to the diffraction of K_{β} line on (400) cubic GaAs crystal plane in DWELLs with QDs grown at 470 (1), 490 (2), 510 (3), 525(4) and 535 °C (5).

Figures 14 presents the superposition of XRD peaks related to the diffraction of $K_{\alpha 1}$ and $K_{\alpha 2}$ lines of the X-ray Cu source from the (200) crystal planes of cubic GaAs substrate and GaAs

layers in studied $In_{0.15}$ $Ga_{0.85}As$ /GaAs QWs. As one can see the peaks (31.69-31.70^o and 31.77-31.78^o) related to the diffraction of $K_{\alpha 1}$ and $K_{\alpha 2}$ lines from the (200) crystal planes in GaAs QW layers with QDs grown at 490-525 ^{o}C locate more close to the corresponding XRD peaks (31.63^o and 31.71^o [22]) of the bulk cubic GaAs (Fig.14). The last fact indicates that the level of elastic strain in $In_{0.15}$ $Ga_{0.85}As$/GaAs QWs of #2, #3, #4 is smaller than in the structures #1 and #5.

In the QD structures with QDs grown at 470 and 535 ^{o}C the corresponding XRD peaks shift to higher angles (31.72^o for $K_{\alpha 1}$ and 31.80^o for $K_{\alpha 2}$) testifying the higher levels of compressive strain in the QWs of structures #1 and #5 (Fig.14). The lowest integrated PL intensities have been detected in the QD structures #1 and #5, apparently, due to the high concentration of nonradiative (NR) defects. The high level of elastic strain enhances, apparently, partial stress relaxation in the structures #1 and #5 that accompanies by the appearance of NR defects.

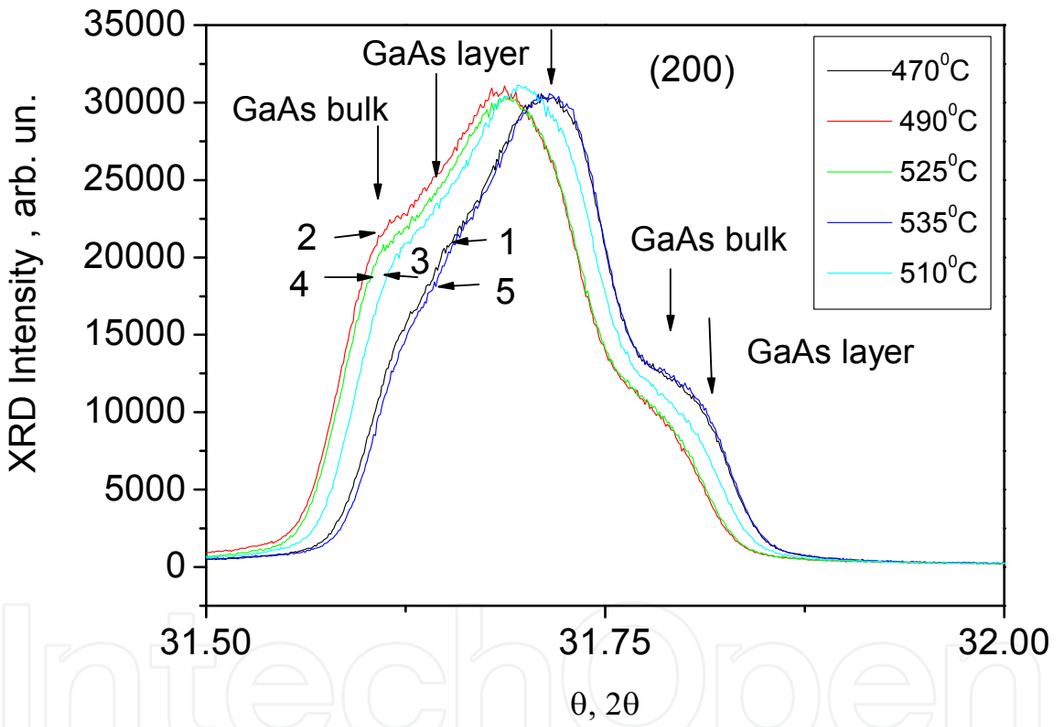

Fig. 14. XRD peaks related to the diffraction of $K_{\alpha 1}$ and $K_{\alpha 2}$ lines of the X-ray Cu source from the (200) crystal planes in the GaAs substrate and GaAs QW layers of studied structures: 1- #1, 2- #2, 3- #3, 4-#4 and 5 - #5.

12. Elastic strain in symmetric InAs QD structures with different QD densities

Let us to discuss the reason of quality changes in studied DWELL structures. It is essential that the application of the buffer and capping $In_xGa_{1-x}As$ layers coupled with InAs QDs stimulates the lattice mismatch and stress decreasing in the vicinity of QDs, but simultaneously to enhance the lattice mismatch and stress increasing at the InGaAs /GaAs interface for the surface area between QDs. With reducing the QD density versus growth

temperature the surface area of QDs reduces (Table 1) and the InGaAs/GaAs interface area between the QDs enlarges. The variation non-monotonically of the integrated PL intensity versus QD density in studied structures, apparently, is connected with the competition of mentioned above two effects.

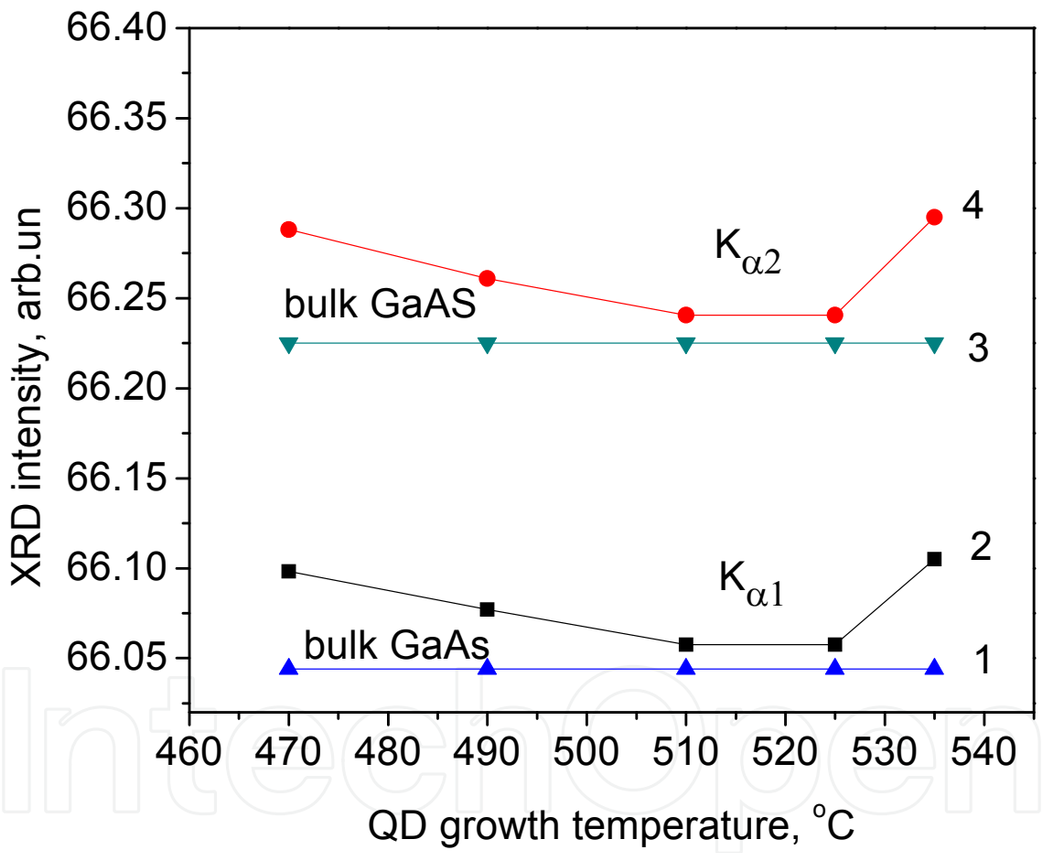

Fig. 15. The 2Θ angles for the diffraction of $K_{\alpha 1}$ and $K_{\alpha 2}$ lines from the (400) crystal planes of the GaAs substrate and GaAs QW layers in DWELLs with QD grown at different temperatures (or with different QD densities).

The X-ray difraction results confirm the mentioned explication. It is knom that the value of elastic deformation can be estimated by following [62]:

$$\varepsilon = -(\theta - \theta_o)\cot\theta_o \,, \tag{10}$$

where Θ and Θ_o are the diffraction angles: in the strained layer (Θ) and in the reference layer without strain (Θ_o). The Θ_o value in present cases has been choosen as the diffraction angle meaning in the bulk cubic GaAs [61]. Thus in studied structures the elastic deformation (or elastic strain) is proportional to the difference between the diffraction angles measured for the GaAs QW layers and the bulk GaAs (Fig.15). Actually as it follows from Fig.15 the variation of elastic deformation in studied structures versus QD growth temperatures (QD densities) has the non monotonous behavior: decreasing in the structures #2, #3 and #4 and increasing in the structures #1 and #5 [38].

Note, that in #3, #4 and #5 the shift of the dependence of PL intensity versus PL peak position into the high energy range (Fig.7) can be explained as well by elastic strain increasing with the enlargement of QD growth temperatures. The high level of elastic strain enhances, apparently, stress relaxation partially in the low quality structures #1 and #5 with the appearance of NR defects (NR1 and NR2) in the GaAs barriers and InGaAs QWs respectively. Simultaneously the shift of GS PL peak to high energy in #5 with larger QD lateral sizes (Table 1) is the subsequence of essential compressive strain in this structure. Note that the compresive strain can stimulate the Ga/In inter-diffusion process in #1 and #5 that is accompained by the PL peak shift into high energy side as well (Fig.7) [63,64].

The low PL intensity in #1 can related to coupling and/or the coalescence of QDs (revealed by AFM for highest concentration of QDs) which can stimulate the NR defect generation, as well as the activation of exciton (or electron/hole) tunneling between the QDs [38]. Finally, the structures with less levels of elastic strain (#2, #3 and #4), have been characterized by the high PL intensity (Fig.3a) and by the shift of GS PL peak emission in low energy spectral range (Fig.2).

13. Conclusions

The photoluminescence, its temperature and power dependences as well as PL inhomogeneity and X ray diffraction has been studied in the symmetric $In_{0.15}Ga_{1-0.15}As$/GaAs quantum wells coupled with InAs quantum dots. The different QD densities in DWELLs were achieved by the variation of QD growth temperatures between 470 and 535 °C. It is shown four reasons for the variation of emission intensities, PL peak positions and PL inhomogeneity in studied QD structures: i) the high concentration of nonradiative recombination centers in the capping $In_{0.15}Ga_{1-0.15}As$ layer at low QD growth temperatures (470°C), ii) the QD density and size distributions along the wafer for DWELLs with QD grown at 510-535°C, ii) the high concentration of nonradiative recombination centers in the GaAs barrier at the QD growth temperature of 535°C and iv) the non monotonous behavior of elastic strain in DWELLs versus QD density. XRD testifies that with decreasing the density of QDs from 1.1 10^{11} cm^{-2} down to 1.3 10^{10} cm^{-2} the level of compressive strain in DWELLs varies not monotonously. The DWELLs with

minimum of elastic strain (#2, #3 and #4) are characterized by the higher PL intensity and by the shift of PL peak to 1.3μm (300K) that is important for the application in optical fiber lasers.

14. Acknowledgements

The work was supported by CONACYT Mexico (project 130387) and by SIP-IPN, Mexico. The author thanks Dr. A. Stintz from Center of High Technology Materials at University of New Mexico, Albuquerque, USA, for growing the studied QD structures and Dr. G. Gómez Gasga for XRD measurements.

15. References

[1] D. Bimberg, M. Grundman, N. N. Ledentsov, Quantum Dot Heterostructures, Ed. Wiley & Sons (2001) 328.
[2] V. M. Ustinov, N. A. Maleev, A. E. Shukov, A. R. Kovsh, A. Yu .Egorov, A. V. Lunev, B. V. Volovik, I. L. Krestnikov, Yu. G. Musikhin, N. A. Bert, P. S. Kopev, Zh .I. Alferov, N. N. Ledentsov, D. Bimberg, Appl.Phys.Lett. 74, 2815 (1999).
[3] G. T. Liu, A. Stintz, H. Li, K. J. Malloy and L. F. Lester, Electron Lett, 35, 1163 (1999).
[4] Stintz, G. T. Liu, L. Gray, R. Spillers, S. M. Delgado, K. J. Malloy, J. Vac. Sci.Technol. B. 18(3), 1496 (2000).
[5] T. V. Torchynska, J. L. Casas Espínola, E. Velazquez Losada, P. G. Eliseev, A. Stintz, K. J. Malloy, R. Peña Sierra, Surface Science 532, 848 (2003).
[6] Y. T. Dai, J. C. Fan, Y. F. Chen, R. M. Lin, S. C. Lee, H. H. Lin, J. Appl. Phys. 82, 4489 (1997).
[7] M. A. Kapteyn, M. Lion, R. Heitz, and D. Bimberg, P. N. Brunkov, B. V. Volovik, S. G. Konnikov, A. R. Kovsh, and V. M. Ustinov, Appl. Phys. Lett. 76, 1573 (2000)
[8] A. Duarte, E. C. F. da Silva, A. A. Quivy, M. J. da Silva, S. Martini, J. R. Leite E. A. Meneses and E. Lauretto, J. Appl. Phys., 93, 6279 (2003).
[9] X.Q. Meng, B. Xu, P. Jin, X.L. Ye, Z.Y. Zhang, C.M. Li, Z.G. Wang, Journal of Crystal Growth 243, 432 (2002).
[10] L. Seravalli, P. Frigeri, M. Minelli, P. Allegri, V. Avanzini, S. Franchi, Appl. Phys. Lett. 87, 063101 (2005).
[11] I. Lubyshev, P. P. Gonzalez-Borrero, E. Marega, Jr. E. Petitprez, N. La Scala, Jr. and P. Basmaji, Appl. Phys. Lett. 68, 205 (1996).
[12] C. Lobo, R. Leon, S. Marcinkevičius, W. Yang, P. C. Sercel, X. Z. Liao, J. Zou, and D. J. H. Cockayne, Phys. Rev. B 60, 16647 (1999).
[13] M. Grundmann and D. Bimberg, Phys. Rev. B 55, 9740 (1997).
[14] W. H. Chang, T. M. Hsu, N. T. Yeh, and J. I. Chyi, Phys. Rev. B 62, 13040 (2000).
[15] J. W. Tomm, T. Elsaesser, Y. I. Mazur, H. Kissel, G. G. Tarasov, Z. Y. Zhuchenko, and W. T. Masselink, Phys. Rev. B 67, 045326 (2003).
[16] T. E. Nee, Y. F. Wu, Ch. Ch. Cheng, and H. T. Shen, J. Appl. Phys. 99, 013506 (2006).

[17] T. V. Torchynska, J. L. Casas Espinola, L. V. Borkovska, S. Ostapenko, M. Dybic, O. Polupan, N. O. Korsunska, A. Stintz, P. G. Eliseev, K. J. Malloy, J. Appl. Phys., 101, 024323 (2007).
[18] S. Sanguinetti, M. Henini, M. Grassi Alessi, M. Capizzi, P. Frigeri, S. Franchi, Phys. Rev. B 60, 8276 (1999)
[19] C. Le Ru, J. Fack and R. Murray, Rhys. Rev. B. 67, 245318 (2003).
[20] S. Khatsevich, D. H. Rich, E.T. Kim and A. Madhukar, J. Appl. Phys. 97, 123520 (2005).
[21] Yu. I. Mazur, B. L. Liang, Zh. M. Wang, D. Guzun, G. J. Salamo, Z. Ya. Zhuchenko and G. G. Tarasov, Appl. Phys. Lett., 89,151914 (2006).
[22] Bacher, C. Hartmann, H. Schweizer, T. Held, G. Mahler, H. Nickel, Phys. Rev. B. 47, 9545 (1993).
[23] T. V. Torchynska, M. Dybiec, S. Ostapenko, Phys. Rev. B. 72, 195341 (2005).
[24] Guffarth, R. Heitz, A. Schliwa, O. Stier, A. R. Kovsh, V. Ustinov, N. N. Ledentsov, D. Bimberg, phys. stat. sol. (b) 224, 61 (2001).
[25] S. Sauvage, P. Boucaud, J. M. Gerard, V. Thierry-Mieg, J. Appl. Phys. 84, 4356 (1998).
[26] S.-K. Eah, W. Jhe, Y. Arakawa, Appl. Phys. Lett. 80, 2779 (2002).
[27] M. Dybiec, L. Borkovska, S. Ostapenko, T. V. Torchynska, J. L. Casas Espinola, A. Stintz and K. J. Malloy, Photoluminescence scanning on InAs/InGaAs Quantum Dot Structures, Applid. Surface Science, 252, 5542 (2006).
[28] M. Dybiec, S. Ostapenko, T. V. Torchynska, E.Velasquez Lozada, P. G. Eliseev, A. Stintz, K. J. Malloy, Photoluminescence mapping on InAs/InGaAs dot structures, phys. stat. sol. (c), 2, n.8, 2951-2954 (2005).
[29] M. Dybiec, S. Ostapenko, T. V. Torchynska, E.Velasquez Losada, Scanning Photoluminescence Spectroscopy in InAs/InGaAs Quantum Dot Structures, Appl. Phys. Lett. 84, 5165-5167 (2004).
[30] M. Catalano, A. Taurino, M. Lomescolo, L. Vasanelli, M. De Giorgi, A. Passasco, R. Rinaldi, R. Cingolani, J. Appl. Phys. 87, 2261 (2000).
[31] Y. Temko, T. Siziki, K. Jacobi, Appl. Phys. Lett. 82, 2142 (2003).
[32] S.E.J. Jacobs, M. Kemerink, P.M. Koenroad, M. Hopkinson, H.W.M. Salimink, J.H. Walter, Appl. Phys. Lett. 83, 290 (2003).
[33] T.V. Torchynska, J. Appl. Phys., 104, 074315 , n.7 (2008).
[34] T.V. Torchynskaa,, A. Vivas Hernandezb, G. Polupanb, E. Velazquez Lozada, Photoluminescence study and parameter evaluation in InAs quantum dot-in-a-well structures, Material Science and Engineering B. 176 , 331–333 (2011).
[35] L.V. Asryan, R.A. Suris, Semicond. Sci. Technol. 11, 554 (1996).
[36] T.V. Torchynska, J.L. Casas Espinola, P.G. Eliseev, A. Stintz, K.J. Malloy, R. Pena Sierra, Phys. Status Solidi (a) 195 , 209 (2003).
[37] C. Pryor, Phys. Rev. B 57, 7190 (1998).
[38] T.V.Torchynska, A. Stintz, Some aspects of emission variation in InAs quantum dots coupled with symmetric quantum wells, J. Applied Physics, 108, 2, 024316 (2010).
[39] Y.P. Varshni, Physica 34 , 149 (1967).

[40] P.G. Eliseev, H. Li, G.T. Iu, A. Stintz, T.C. Nevell, L.F. Lester, J. Mally, IEEE J. Select. 35 Topics Quant. Electron. 7 (3) (2001) 135.
[41] Y.S. Huang, H. Qiang, F.H. Pollack, G.D. Pettit, P.D. Kirtchner, J.M. Woodall, H. Stagier, L.B. Soresen, J. Appl. Pys. 70 (12) (1991) 7537
[42] Torchynska, T.V., Casas Espinola, J.L., Lopez, H.M.A., Eliseev, P.G., Stintz, A., Malloy, K.J., Pena Sierra, R. *Institute of Physics Conference Series,* 174, 69-71 (2003).
[43] J. L. Casas Espinola, M. Dybiec, S. Ostapenko, T. V. Torchynska and G. Polupan, J. of Physics: Conference Series, 61, 180-184 (2007).
[44] L. Casas Espinola, 1 T. V. Torchynska, G. Polupan, R. Pena Sierra, phys. stat. sol. (c), 4, n.2, 379-381 (2007).
[45] M. De Giorgi, C. Lingk, G. von Plessen, J. Feldmann, S. De Rinaldis, A. Passaseo, M. De Vittorio, R. Cingolani, M. Lomascolo, Appl. Phys. Lett. 79, 3968 (2001).
[46] S. Marcinkevicius, R. Leon, Phys. Rev. B., 59, 4630 (1999).
[47] B. Ohnesorge, M. Albrecht, J. Oshinowo, A. Forchel, Y. Arakawa, Phys. Rev. B., 54, 11532 (1996).
[48] T.V. Torchynska, E. Velazquez Lozada, J.L. Casas Espinola, J. Vac. Scien. & Tech. B 27(2), 919-922, (2009)
[49] T.V. Torchynska, Superlattice and Microstructure, 45, 349-355 (2009)
[50] T. V. Torchynska, J. L. Casas Espinola, E. Velasquez Lozada, L. V. Shcherbyna, A. Stintz, R. Pena Sierra, Localization of defects in InAs QD symmetric InGaAs-GaAs DWELL structures, Physica B: Condensed Matter, 401-402, 584-586 (2007), ISSN 0921-4526.
[51] E. Zhukov, A. R. Kovsh, N. A. Maleev, S. S. Mikhrin, V. M. Ustinov, A. F. Tsatsulnikov, M. V. Maximov, B. V. Volovik, D. A. Bedarev, Y. M. Shernyakov, P. S. Kopev, Z. I. Alferov, N. N. Ledentsov, D. Bimberg, Appl. Phys. Lett. 75, 1926 (1999).
[52] K. Nishi, H. Saito, S. Sugou, J. S. Lee, Appl. Phys. Lett. 74, 1111 (1999).
[53] N. T. Yeh, T. E. Nee, J. I. Chyi, T. M. Hsu, C. C. Huang, Appl. Phy. Lett. 76, 1567 (2000).
[54] F. Guffarth, R. Heitz, A. Schliwa, O. Stier, N. N. Ledentsov, A. R. Kovsh, V. M. Ustinov, D. Bimberg, Phys. Rev. B, 64, 085305 (2001).
[55] E. Romanov, G. E. Beltz, W. T. Fischer, P. M. Petroff, J. S. Speck, J. Appl. Phys., 89, 4523 (2001).
[56] Y. Y. Lin, J. Singh, J. Appl. Phys. 92, 6205 (2002).
[57] B. Yang, J. Appl. Phys. 92, 3704 (2002).
[58] Y. Nabetani, T. Matsumoto, G. Sasikala, I. Suemune, J. Appl. Phys. 98, 063502 (2005).
[59] T.V.Torchynska, J. Palacios Gomez, G. Gomez Gasga, A. Vivas Hernandez, E. Velazquez Lozada, G. Polupan, Ye. S. Shcherbyna, J. of Physics, Conference Ser. 245, 012060 (2010).
[60] J.L. Casas Espinola, T V Torchynska, J Palacios Gomez, G Gómez Gasga, A Vivas Hernandez and R. Cisneros Tamayo, phys.stat.solid. (c). 8, No. 4, 1391-1393 (2011)
[61] Yeh CY, Lu ZW, Froyen S and Zunger A, *Phys. Rev.* B, 46, 10086 (1992).
[62] S. Ejiri, T. Sasaki, and Y. Hirose, Thin Solid Films 307, 178 (1997)

[63] J. L. Casas Espínola, T. V. Torchynska, G. Polupan, and M. Ojeda Martínez, phys.stat.solid.(c) 8, No. 4, 1388–1390 (2011)
[64] J. Casas Espinola, V. Torchynska, G 1 . Polupan, E. Velazquez Lozada, Material Science and Engineering, B., 165, 115- 117 (2009)

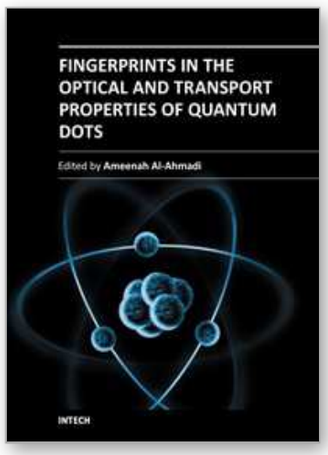

Fingerprints in the Optical and Transport Properties of Quantum Dots

Edited by Dr. Ameenah Al-Ahmadi

ISBN 978-953-51-0648-7
Hard cover, 468 pages
Publisher InTech
Published online 13, June, 2012
Published in print edition June, 2012

The book "Fingerprints in the optical and transport properties of quantum dots" provides novel and efficient methods for the calculation and investigating of the optical and transport properties of quantum dot systems. This book is divided into two sections. In section 1 includes ten chapters where novel optical properties are discussed. In section 2 involve eight chapters that investigate and model the most important effects of transport and electronics properties of quantum dot systems This is a collaborative book sharing and providing fundamental research such as the one conducted in Physics, Chemistry, Material Science, with a base text that could serve as a reference in research by presenting up-to-date research work on the field of quantum dot systems.

How to reference

In order to correctly reference this scholarly work, feel free to copy and paste the following:

Tetyana V. Torchynska (2012). InAs Quantum Dots in Symmetric InGaAs/GaAs Quantum Wells, Fingerprints in the Optical and Transport Properties of Quantum Dots, Dr. Ameenah Al-Ahmadi (Ed.), ISBN: 978-953-51-0648-7, InTech, Available from: http://www.intechopen.com/books/fingerprints-in-the-optical-and-transport-properties-of-quantum-dots/inas-quantum-dots-in-symmetric-ingaas-gaas-quantum-wells

INTECH
open science | open minds

InTech Europe
University Campus STeP Ri
Slavka Krautzeka 83/A
51000 Rijeka, Croatia
Phone: +385 (51) 770 447
Fax: +385 (51) 686 166
www.intechopen.com

InTech China
Unit 405, Office Block, Hotel Equatorial Shanghai
No.65, Yan An Road (West), Shanghai, 200040, China
中国上海市延安西路65号上海国际贵都大饭店办公楼405单元
Phone: +86-21-62489820
Fax: +86-21-62489821

IntechOpen